Proceedings of 10th International Conference on Precision, Meso, Micro and Nano Engineering (COPEN 10)
December 07 – 09, 2017, Indian Institute of Technology Madras, Chennai – 600 036 INDIA

A Study of the Wear Behavior of A2024-SiC-$ZrSiO_4$ Metal Matrix Composites with Fine Silica Slurry Particles

[1]Surendra Kumar Patel, [2]Virendra Pratap Singh, [3]Raman Nateriya, [4]Kuriachen B

[1]Research Scholar, Department of Mechanical Engineering, NIT Mizoram, India
[2]Research Scholar, Department of Mechanical Engineering, NIT Mizoram, India
[3]Assistant Professor, Department of Civil Engineering, MANIT, Bhopal, India
[4]Assistant Professor, Department of Mechanical Engineering, NIT Mizoram, India

Abstract

This paper is a comparative study of dual reinforcement particles with combination of various weight ratio of reinforcement on microstructural features and slurry erosive wear behavior in A2024 alloy. Silicon carbide of (35-44 µm) and zircon sand particles of (20-35 µm) are reinforced in the alloy by two-step stir casting method. Slurry erosive wear study revealed that the 1:3 ratio (zircon sand and silicon carbide) of dual particle reinforcement enhances the wear resistance as compared to other weight percentage (1:1, 3:1) of dual particle reinforcement if mixed in a definite proportion. The wear behavior was examined by the sample rotation technique using slurry pot erosion tester. The effects of speed, slurry media and sand concentration on the slurry wear behavior have been studied. To examine the influence of the SiC and $ZrSiO_4$ particle dispersion matrix alloy was also characterized under similar conditions. It was observed that the addition of SiC and $ZrSiO_4$ significantly improves the wear resistance of the matrix alloy in marine and mine environment and wear rate increases with slurry volume content. However, slurry environment and speed has a mixed effect on the wear rate. Study also indicate that a combination of 12 % reinforcement of zircon sand and silicon carbide particles in the ratio of 1:3 into the composite exhibits better erosive wear resistance as compared to other combinations.

Keywords: A2024 alloy, silicon carbide, zircon sand, fine silica quartz sand, slurry erosion tester TR-40.

1. INTRODUCTION

Aluminum alloy matrix composites (AMCs) with multiple reinforcements or hybrid AMCs are finding increased applications in various sectors because of improved mechanical and tribological properties and hence are better substitutes for single reinforced composites [1, 2]. Aluminum and its alloys when reinforced with hard ceramic particulates impart a combination of properties not achievable in either of the constituents individually. Aluminium alloys provide a good matrix for the development of particulate reinforced composites owing to their low density, high specific strength, high corrosion resistance, ease of fabrication, and low cost [3].

In recent years many processing techniques have been developed to prepare particulate reinforced aluminium matrix composites. Among the variety of processing techniques available for particulate or discontinuous reinforced metal matrix composites, stir casting is one of the methods accepted for the production of large quantity composites. It is attractive because of simplicity, near net shaping, flexibility and is most economical for large size components to be fabricated. However, it suffers from poor distribution of the reinforcement particles in the aluminum matrix composite. These problems become especially significant as the reinforcement size decreases due to greater agglomeration tendency and reduced wettability of the particles with the melt [3–6]. The dendritic growth and porosity also exists in stir cast composites. Therefore, innovations in processing method of stir casting are of great importance. Stir casting process is modified by various researchers to achieve the desired properties in the composite [7–11]. Two-step stir casting has an advantage in terms of promoting wettability, reduction of porosity, and homogeneous distribution of particles. Moreover, the microstructure is also refined which provide better mechanical properties [9, 10]. In earlier reported two-step stir casting method the mixing of particle is done in semisolid melt by manually stirring with steel rod, which is cumbersome process and also the agglomeration of fine particles occurs. Moreover, mixing is not efficient in reinforcement of fine particle as total volume occupied is increased and semisolid melt solidifies before mixing is completed. In recent year numerous research works have been reported on production of multi particle reinforced or hybrid AMCs reinforced with TiC, $ZrSiO_4$, and graphite or in combination of the above, but very limited research work has been done on reinforcement of dual hard particles [2, 11, 12, and 13]. Moreover, no work is reported on slurry erosion wear behavior of A2024, aluminum alloy composites fabricated by stir casting and reinforced with silicon carbide (44-60 µm) and zircon sand particles (20-30 µm) [14].

Another study shows the dry sliding wear behavior of Al-matrix composites reinforced with zircon sand and SiC particulate up to 12 %. Study shows that A2024 alloy/SiC/$ZrSiO_4$ hybrid composite exhibited better wear resistance but optimal addition of graphite particles is necessary. Metal–metal and metal–abrasive wear tests revealed that wear resistance of the composites increased with increasing Mg addition [1].

The present study is aimed to analyze the combined effect of both the hard particles (SiC and $ZrSiO_4$) reinforcement in A2024 alloy composite fabricated by modified two-step stir casting.

In first step the melting and mixing is done properly as is being followed in stir casting and melt is solidified in crucible. In the second step the solidified mass is re-melted for stirring process followed by casting. We investigated the room temperature sliding wear behaviors of reinforced aluminium matrix hybrid composites under both the dry and lubricant conditions. Study shows that wear behavior are related to the fiber orientation of alumina fiber both in dry and lubricated conditions.

ISBN: 978-93-80689-28-9

Table 1. Composition of the A2024 alloy in wt. %.

A2024 alloy	Si	Cu	Cr	Fe	Zn	Ti	Al
Wt.%	0.5	3.8-4.9	0.1	0.5	0.25	0.15	Balance

2. MATERIALS SELECTION AND EXPERIMENTAL PROCESSES

In the present investigation, well-known piston alloy A2024 is used as matrix material and high purity zircon sand ($ZrSiO_4$) and silicon carbide (SiC) as reinforcement. A2024 alloy was obtained in the form of ingots. The chemical compositions of the A2024 alloy are given in Table 1. The composite was made by stir casting route.

Table 2. List of processing parameters.

Parameters	1st steps	2nd steps
Melting temperature	800^{0}C	850^{0}C
Total stirring time	20mim	4min
Mixing time	8min	12–15 min
Blade angle	45^0	45^0
No of blade	4	4
Position of stirrer	Up to 2/3 depth in the melt	Up to 2/3 depth in the melt

Required quantity of A2024 alloy was taken in a graphite crucible and melted in an electric furnace. The temperature of melt was raised to 850 ^{0}C. This molten metal was stirred using a graphite impeller at a speed 630 rpm. At this 630 rpm vortex is created in the melt, which facilitate to suck the reinforced particles inside the melt.

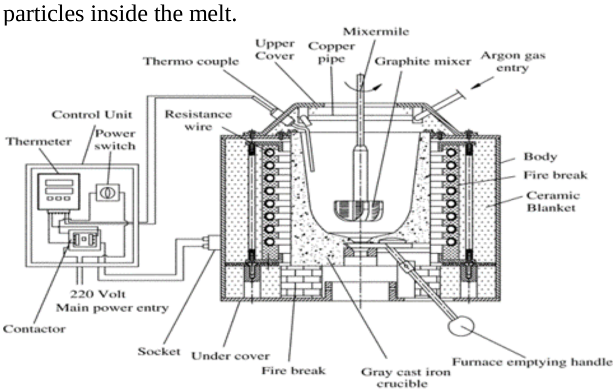

Fig 1. Stir casting processes

The ceramic particles used as reinforcement were taken in defined proportion and mixed properly by spatula. Particles prior to mixing were preheated at 450^0 C to off the moisture. After the formation of vortex in the melt, the particles were charged inside the vortex at the rate of 20–25 g/min into the melt during stirring by impeller with the help of funnel kept on top of vortex. Zircon sand and silicon carbide particles of fine grade were selected for present work. After mixing of particles the melt slurry is allowed to solidify in a graphite crucible at room temperature conditions. After solidification the mixture is again re-melted in a furnace to ensure that slurry is in fully liquid condition and then melt is stirred with impeller for 12–15 min. similar type of synthesis of composite was reported earlier by various researchers [7, 10 and11]. During production of composite, the amount of A2024 alloy, stirring duration and position of stirrer in the crucible were kept constant to minimize the contribution of variables related to stirring on distribution of second phase particles. The other detail of it is given in Table 2. In our earlier work it is observed that 12 % reinforcement of zircon sand reinforced composite has given better property.

Table 3. Combination of reinforcement composites.

Composite	Total 15wt% reinforcements	
	Silicon carbide (SiC)	Zircon sand ($ZrSiO_4$)
A	9	3
B	6	6
C	3	9

In order to compare and correlate the effect of dual particle reinforcement on mechanical and tribological properties, three different composites containing a total of 12wt% reinforcement in different proportion were fabricated and have been designated by alphabets. The reinforcement combinations are also given in Table 3.

2.1 Mechanical Properties of Zircon Sand and silicon carbide Particles

2.1.1 Zircon Sand

Zircon sand consists of mostly zirconium silicate ($ZrSiO_4$) and some hafnium in addition to some rare earth elements, titanium minerals, monazite, etc. Zirconium was found to be a promising candidate as reinforcement material for aluminium, zinc and lead based composites [2].

Table 4. Chemical compositions of zirconium sand

Composition	ZrO_2	SiO_2	HfO_2	Al_2O_3	Fe_2O_3	MgO
(Wt. %)	67.22	30.85	1.39	0.11	0.029	0.014

2.1.2 Silicon Carbide

Silicon Carbide is the only chemical compound of carbon and Silicon. It is used in abrasives, refractories, ceramics, and numerous high-performance applications. Silicon Carbide crystal structure is Octahedral [3].

Table 5. Mechanical properties of Titanium carbide and zircon sand.

Properties	**Silicon Carbide**	**Zircon sand**
M.P. (^{0}c)	2830	2500
Limit of application (^{0}c)	1400-1700	1870
Linear coeff. of expansion (10^{-6k})	4.1-7.7	7.5
Density g/cm^3	3.16	4.5-4.7
Hardness (kg/mm^2)	2800	4.5
Fracture toughness(MPa-m$^{1/2}$)	4.6	5
Crystal structure	Hexagonal	Tetragonal

2.2 Microstructure

The microstructural analysis has been completed with the help of scanning electron microscope (JEOL, JSM-6390A, Japan) at various magnifications. Before optical observation the sample was mechanically polished and etched by Keller's reagent for obtaining better contrast.

2.3 Microhardness

Micro hardness of the different phases was measured (Mitutoyo, japan) using micro hardness tester in MANIT, Bhopal. Micro hardness measurement was done on each set of sample by taking minimum of five indentations per sample at 100 kg load.

2.4 Slurry Erosion Wear Test

Slurry erosion wear tests of the reinforced alloys composite were performed at 'Slurry Erosion Tester TR-40, under the room temperatures between 25 and 30 ^{0}C. Before testing, each specimen was ultrasonically cleaned in acetone. The wear tests of specimen from each set of composite have been conducted at the 500, 1000, 1500 rpm and at three different slurry concentration of coarse silica quartz sand 25%, 50%, 75% by wt% and water by wt% in gram (gms). The test specimens of size 76.5x25.4x6.35 mm were metallographically prepared and polished. Coarse silica quartz sand: AFS 40/30 mesh sizes were used as slurry. Test duration of one hour was adopted for all specimens. Using digital weighting machine of accuracy 0.1 mg wear was measured.

3. RESULTS AND DISCUSSION

3.1. Microstructure Analysis

The SEM micrograph of the composites is shown in Fig. 2a–c. The micrograph clearly reveals the absence of dendritic morphology in all the composites under investigation. The dendritic structure can be modified during casting which is influenced by many factors such as dendritic fragmentation, restriction of dendritic growth by the particles, and thermal conductivity mismatch between the particles and melt. Dendritic fragmentation can be attributed to the shearing of initial dendritic arms by the stirring action. It was also found that the perturbation in the solute field due to the presence of particles can change the dendrite tip radius and the dendrite tip temperature. These effects give rise to a dendrite to cell transition as the density of particles is increased. Also the length of the dendrite is reduced in the presence of the particles. Ceramic particle also act as a barrier for dendritic growth and this phenomena is more pronounced if the cooling rate is high. In this work it is reported that the particle can be assumed to act as a barrier to the dendritic growth. And this phenomenon is more pronounced if the cooling rate is high.

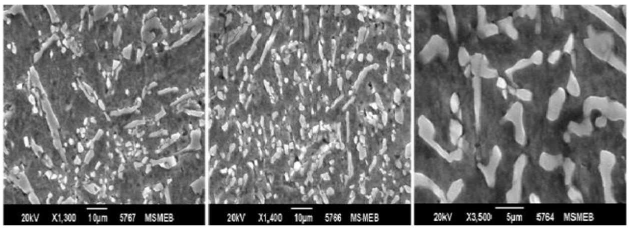

a) b) c)

Fig 2. The SEM images, a composite A, b composite B, c composite C.

It is also reported in work that the growing dendrite tip realizes the existence of a hot liquid front near the particle as thermal conductivity of particle is low, which in turn retards its further growth. The needle or acicular eutectic silicon morphology can be seen (Fig. 2a). However, non-acicular morphology in the vicinity of the particle and arranged in colonies are also observed Fig. 2(b-c). This is attributed to the fact that particles are effective nucleation site for eutectic silicon and also the thermal conductivity difference between particle and alloy matrix creates thermal gradient at interface. Ceramic particles have a lower thermal conductivity and heat diffusivity than those of aluminum melt. Therefore, particles are unable to get cooled at faster rate as compared to the melt. As a result, the temperature of the particles is always higher than the liquid alloy. The hotter particles may heat up the liquid in their immediate surroundings and thus delay solidification of the surrounding liquid alloy. This thermal mismatch causes nucleation of phase in the liquid alloy at a distance away from the particles, where the temperature is lower. The growth of the nuclei will lead to enrichment of silicon in the remaining melt zone. Si crystals composite were observed to nucleate from particles as freezing point of silicon is high. This heterogeneous nucleation can be explained as a result of enrichment of silicon in the melt around the particles. In the images Fig. 2(a-c) reinforcement of silicon is also observed. The refinement of silicon is more pronounced in the composites containing silicon carbide particles which increase with the increase in its content. In addition to this, morphology of eutectic silicon gets modified in presence of SiC particles. Similarly, finding on refinement and morphological feature of eutectic silicon in the presence of silicon carbide particles is reported [15]. The SEM image of composite 'A' reinforced with 12 % of zircon sand and SiC particles in the ratio of 1:3 are shown in Fig. 2(a-c). Refined microstructure and absence of dendritic morphology can be attributed to the two-step stir casting process adopted here in which prolonged time of mixing and stirring is bifurcated. Colonies of eutectic silicon are arranged in the vicinity of the particle. Moreover, near the particle, eutectic silicon having globular morphology or blunted morphology as compared to the matrix can be seen. Each and every particle is having a colony of eutectic silicon which is indicative of the role of particles in nucleating the eutectic silicon. Zircon sand and SiC particles provide effective site for nucleation and also restricts the growth of dendrite and modifies the matrix with more refined structure leading to improvement in strength. The distribution of eutectic silicon is also refined in the matrix alloy. Similarly morphological transformation attributed to the localized rapid cooling effect produced by particles due to large temperature difference in the melt around its vicinity.

The SEM image of composite 'B' containing 12 % of SiC and zircon sand particles in the ratio of 1:1 are shown in Fig. 2(a-c). It depicts the refinement of microstructure and eutectic silicon. Eutectic silicon along with dispersed particles is densely arranged in such a way that they cover almost the entire matrix. The eutectic silicon refines to finer scale and nucleates near particles as colonies. Clustering of particles is observed at some places and some of the clustered particles have chipped out during polishing the samples. However, fine particles have the tendency of clustering though it is not much pronounced in the prepared composites.

The SEM image of composite 'C' containing 12 % of zircon sand and SiC particles in the ratio 2:1 is shown in Fig. 2(a-c). Finer to coarse distribution of eutectic silicon along with homogeneous distribution of particles can be seen. Eutectic silicon colonies around particle are more pronounced in the micrograph. Eutectic silicon distribution is more refined and morphology has changed from acicular to globular around the particles. Also in the matrix the eutectic silicon having blunted morphology as compared to long needle shape or acicular is seen. However, the fine particles and silicon form a network structure because of pushing interface from different nucleation sites. Moreover, the clustering of fine particles at some places is also observed.

Overall analysis of structure indicates that microstructure is refined whereas eutectic silicon are having blunted and globular morphological features. This refinement may lead to better tribological and mechanical properties in the composite. The colonization of eutectic silicon in the vicinity of the particles enhances particle capability of wear resistance. The reinforced particles are uniformly distributed in the alloy matrix. The good bonding between particles and alloy matrix is also revealed in the microstructural analysis. Moreover, porosity is at minimum level and not observed in the optical examination, although clustering is seen at same places in the composite. Microstructure analysis shows that addition of SiC has a pronounced effect on the microstructure and eutectic silicon refinement. The degree of microstructure and eutectic silicon refinement increases in accordance with the increase of SiC-reinforced particle percentage. The most prominent feature observed in all composite is the absence of dendritic growth which is accounted for two-step stir casting processing of the composites.

3.2. Microhardness and density

Micro hardness measurement at different phases of composite has been carried out to know the effect of reinforced particulates on the alloy matrix. This is given in Table 6. Micro hardness measurement has been carried out on the embedded reinforced particles as well as in the vicinity of particles and matrix.

Table 6. Variation of micro hardness (H_v) and density of composite

Composite	Particle	Interface	Matrix	Density g/cm^3
A	251.03	131.38	89.09	2.727
B	178.10	117.81	65.73	2.746
C	194.43	125.91	69.38	2.762

3.3. Slurry erosion wear characteristic on coarse silica quartz sand

Slurry erosion test was performed for 1 hour duration at 500,1000,1500 rpm using fine particle sand at various (25%, 50% and 75%) concentrations and following observations were made.

In above graph enhance the loss of mass at 500, 1000 and 1500 rpm at various slurry concentrations. The comparison of slurry erosion wear behavior of all the composites at different speeds (500, 1000 and 1500rpm) and different slurry concentration (25%, 50% and 75% by weight) on fine sand depicts that wear rate (m/s) increases almost linearly with increase speeds and slurry concentration. It is observed that at low speed and low slurry concentration all the composites exhibit almost similar type of wear behavior. The wear curve trend is almost similar due to speeds and slurry concentration but it is higher for composite B&C and lower for composite ‘A’. Good interfacial bonding of reinforcement with the matrix and higher microhardness as possessed by composite a results better wear behavior.

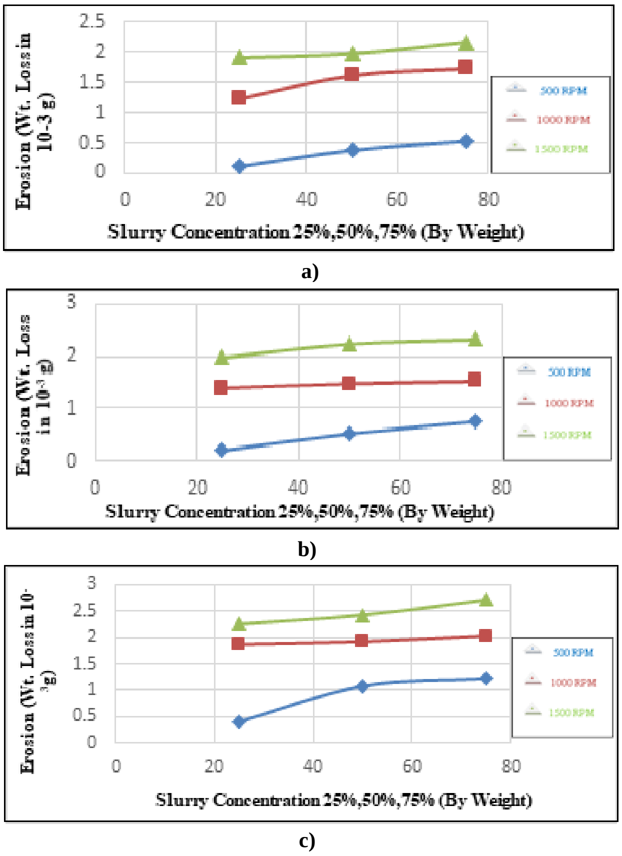

Fig 3. The mass loss of composites a composite A, b composite B, c composite C at one hour rotation in fine sand (25%, 50% and 75% by weight) at 500, 1000 and 1500 rpm

On the other hand, composite ‘A’ shows better wear resistance at coarse silica quartz sand at 500, 1000, and 1500rpm and 25%, 50% and 75% slurry concentration. Wear behavior of composites B & C is nearly similar but run-in wear is higher for composite ‘C’. The composite with equal amount of dual reinforcement, i.e., composite ‘B’ provides better wear properties as compared to composites ‘C’. Also the composite ‘A’ with 9% sliicon carbide and 3% zircon sand shows increase in wear rate as compared to composite B&C. Dual particles have different role in the matrix, silicon carbide particles refines the eutectic silicon whereas zircon sand particles provides good bonding characteristics to the matrix. zircon sand particles as composite A which shows better wear resistance having combination of 9% silicon carbide particles and 3 % zircon sand particles. The composite B is combination of 6% zircon sand and 6% silicon carbide particles shows better wear resistance as compared to composite ‘C’ which is composite ‘C’ having 9% zircon sand and 3% silicon carbide particles.

After analyzing wear behavior of composites, it is clear that dual particle reinforcement mixed in definite proportion is only effective for enhancing wear resistance. Silicon carbide particles are better reinforcement for wear behavior as compared to zircon sand particles. Composite exhibits better wear resistance due to high micro hardness of the interface between particle and matrix.

3.4. Morphological analysis of slurry erosion wear surface

The SEM micrograph of slurry erosion surface of composite 'A' at different rpm and slurry concentrations of fine silica quartz sand is shown in Fig 4. At 500 rpm composite B is showing high wear rate (m/s) as shown in Fig.4a. Long and wider craters along the erosion wear are observed with erosive particles of impact crater. At 1000 rpm the particles of SiCp are reduces in distribution than matrix seems to be softer shown in Fig. 4b. Material removal is excessive as craters become deeper. Flakes of wear surface are also visible in this micrograph, if hard particles distributed over the area than matrix seems to be less soft or matrix become more harder as shown in fig 4. At 1500 rpm the material removal is excessive due to increasing the striking slurry on the composite rpm. The subsurface and surface cracks are visible in Fig. 4c. The crack propagation is along the increasing rpm and slurry concentrations, which result in material removal by delimitation. Several micro cracks are also propagating resulting in the removal of material by delimitation. Rupture of mechanically mixed layer accelerated the removal of material by slurry erosive wear. The particles get deboned which results in increase loss of material.

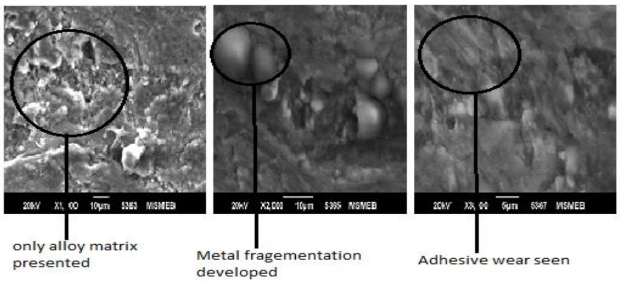

a)

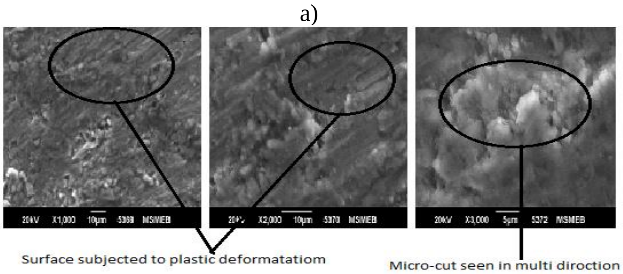

b)

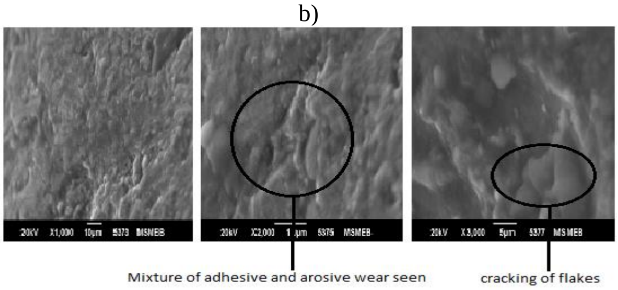

c)

Fig 4. SEM micrograph of wear surface of composite A, a- 500 rpm, b- 1000 rpm, c- 1500 rpm and slurry concentrations of fine silica quartz sand at different magnifications

Slurry concentration loss of materials increases with increase rpm respectively but at 75% slurry concentration loss of materials decrease as compared to, 50% slurry concentrations. Because of at the high speed slurry particle are collides to each other, so impinging rate of slurry on composite decrease, so wear rate also some decrease from composite 'B' but composite 'A' is better wear resistance In this way composite A is better wear resistance as compare to other composite.

The SEM micrograph of slurry erosion surface of composite 'B' at different rpm and slurry concentrations of fine silica quartz sand is shown in Fig 5. At 500 rpm composite 'B' is showing high wear rate (m/s) as shown in Fig. 5a. Long and wider craters along the erosion wear are observed with erosive particles of impact crater. At 1000 rpm the particles of SiCp are reduces in distribution than matrix seems to be softer shown in Fig. 5b. Material removal is increases as craters become deeper. Flakes of wear surface are also visible in this micrograph, if hard particles distributed over the area than matrix seems to be less soft or matrix become more harder as shown in fig. At 1500 rpm the material removal is excessive due to increasing the striking slurry on the composite rpm. The subsurface and surface cracks are visible in Fig. 5c. The crack propagation is increase with the increasing rpm and slurry concentrations, which result in material removal by delimitation. The particles get deboned which results in increase loss of material. This work reported that the first at 25%, to 50% slurry concentration loss of materials increases with increase rpm respectively but at 75% slurry concentration loss of materials decrease as compared to 50% slurry concentrations, because of at the high speed slurry particle are collides to each other, so impinging rate of slurry on composite decrease, so wear rate also some decrease from composite 'B' but composite 'A' is better wear resistance. In this way composite 'A' is better wear resistance as compare to composite 'B'.

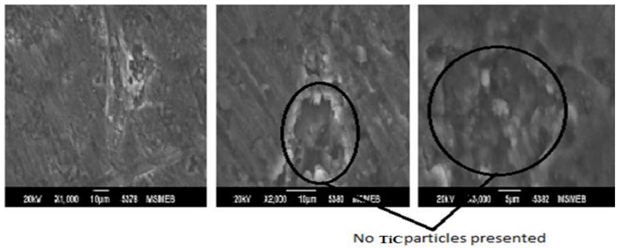

a)

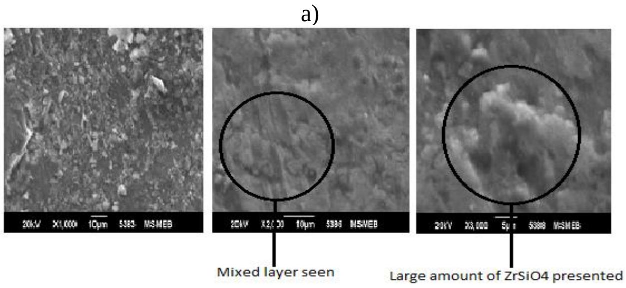

b)

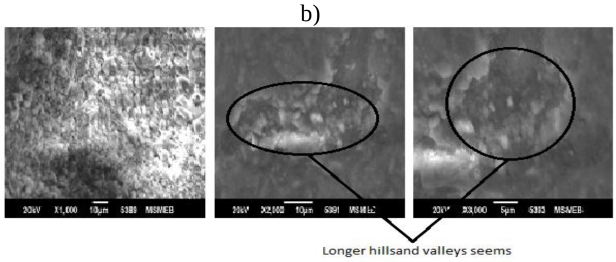

c)

Fig 5. SEM micrograph of wear surface of composite B, a- 500 rpm, b- 1000 rpm, c- 1500 rpm and slurry concentrations of fine silica quartz sand at different magnifications

The SEM micrograph of slurry erosion surface of composite ‘C’ at different rpm and slurry concentrations of fine silica quartz sand is shown in Fig. 6. At 500 rpm composite ‘C’ is showing high wear rate as shown in Fig. 6a. Long and wider craters along the sliding direction are observed with erosive particles of mechanically mixed layer. At 1000 rpm the particles of adhesive and erosive mixed layer is shown in Fig. 6b. Material removal is excessive as craters become deeper. Flakes of wear surface are also visible in this micrograph. At 1500 rpm the material removal is excessive due to high rpm. The subsurface and surface cracks are visible in Fig. 6c. The crack propagation is along the rpm and slurry concentrations, which result in material removal by delimitation. The particles get deboned which results in increase loss of material. we have reported in their work that the first at 25%, to 50% slurry concentration loss of materials increases with increase rpm respectively but at 75% slurry concentration loss of materials decrease as compared to 25%, 50% slurry concentrations. In this way composite A is better wear resistance as compare to composite B and composite ‘C’.

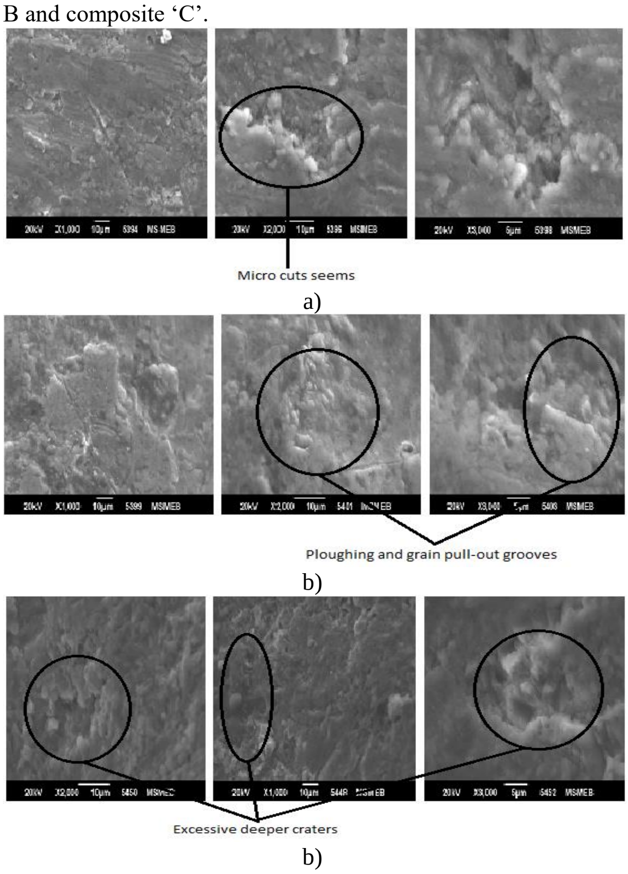

Fig 6. SEM micrograph of wear surface of composite C, a- 500 rpm, b- 1000 rpm, c- 1500 rpm and slurry concentrations of fine silica quartz sand at different magnifications

The comparison of slurry erosion wear behavior of all the composites at different speeds (500, 1000 and 1500rpm) and different slurry concentration (25%, 50% and 75% by weight) on coarse sand depicts that wear rate increases almost linearly with increase speeds and slurry concentration. It is observed that at low speed and low slurry concentration all the composites exhibit almost similar type of wear behavior. The wear curve trend is almost similar due to speeds and slurry concentration but it is higher for composite B&C and lower for composite ‘A’. Good interfacial bonding of reinforcement with the matrix and higher microhardness as possessed by composite, results better wear behavior. On the other hand, composite ‘A’ shows better wear resistance at coarse sand at 500, 1000, and 1500rpm and 25%, 50% and 75% slurry concentration. Wear behavior of composites ‘B’ and ‘C’ is nearly similar but run-in wear is higher for composite ‘C’. The composite with equal amount of dual reinforcement, i.e., composite B provides better wear properties as compared to composites ‘C’. Also the composite with 9 % silicon carbide and 3% zircon sand i.e., composite ‘A’ shows increase in wear resistance as compared to composite B&C. Dual particles have different role in the matrix, silicon carbide particles refines the eutectic silicon whereas zircon sand particles provides good bonding characteristics to the matrix. Composite A which shows better wear resistance having combination of 9% silicon carbide particles, and 3% zircon sand particles. The composite ‘B’ is combination of 6% zircon sand and 6% silicon carbide particles shows better wear resistance as compared to composite ‘C’ which is having 9% zircon sand and 3% silicon carbide particles.

After analyzing the wear behavior of composites, it is clear that dual particle reinforcement mixed in definite proportions only effective for enhancing wear resistance. Silicon carbide particles are better reinforcement for wear behavior as compared to zircon sand particles. Composite ‘A’ exhibits better wear resistance due to high microhardness of the interface between particle and matrix.

4. CONCLUSIONS

The present investigation is carried out to determine the influence of dual particle reinforcement on microharnness; microstructural analysis and slurry erosion wear behavior of stir cast A2024 alloy composites. The comparison of wear behavior and micro structural micro graphs of the fabricated composite following conclusion can be calculated:

1. Aluminium alloys (A2024) composites of various wt% reinforced with SiC and $ZrSiO_4$ particles can be successfully synthesized by stir casting method.

2. Microstructural observations shows that the reinforced particles SiC and $ZrSiO_4$ are uniformly distributed in A2024 aluminium alloy matrix and good interfacial bonding between particles and matrix.

3. The dual particle reinforcement enhances the better erosion wear resistance in A2024 alloy composites.

4. The combination of reinforcement in aluminium alloy composites 9% SiC and 3% zircon sand reinforced particles composite (Composite A) yields better wear resistance as compared to other composites ‘B’ and ‘C’ in A2024 alloy composites.

5. The reinforcement up to 15wt% yields better mechanical properties in A2024 alloy composites. Increasing in speed (rpm) and slurry particle size (fine) increases the erosion and abrasion wear in A2024 alloy composites.

6. The wear rate increases with increasing in slurry concentrations, first at 25% to 50% slurry concentration loss of materials increases with increase rpm respectively but at 75% slurry concentration loss of materials decrease as compared to 25%, 50% slurry concentrations.

5. ACKNOWLEDGEMENTS

The authors are thankful to acknowledge the financial support from Maulana Azad National Institute of Technology Bhopal (M.P.) India.

References

[1] Vipin Singh., Suresh Kumar., Ranvir Singh Panwar., O.P. Panday., “Microstructural and wear behavior of dual reinforced particle (DRP) aluminium alloy composite”, J Mater sci, 47: 6633-6646, 2012.

[2] Suresh Kumar., Ranvir Singh Panwar., O.P. Pandey., “Wear Behavior At High Temperature of Dual-Particle Size Zircon-Sand-reinforced Aluminum Alloy Composite”, The Minerals, Metals & Materials Society And ASM International, 44A: 1548-1565, 2012.

[3] Suresh Kumar., Vipin Sharma., Ranvir Singh Panwar., O. P. Pandey., “Wear Behavior of Dual Particle Size (DPS) Zircon Sand Reinforced Aluminium Alloy”, Tribol Lett, 47: 231–251, 2012.

[4] Girish R. Desale., Bhupendra K. Gandhi., S.C. Jain., “Slurry erosion of ductile materials under normal impact condition”, Wear, 264: 322-330, 2012.

[5] A. Thangarasu A., Murugan N., S.J.Vijay., I. Dinaharan., “Fabrication of AA1050/10wt.% TiC Surface Composite using Friction Stir Processing”, Proceedings of International Conference on Advanced Materials, PSG College of Technology, 277-281, 2012.

[6] L.O. Asuquo., E. N. Bassey., A. P. Ihoms., “Characteristics of zircon sand the effect on foundry casting”, Journal of mechanics & industry research 1(2013), pp. 27-32.

[7] Chandraveer Singh., K. K. S. Mer., “Abrasion wear characterization of Al-Al_2O_3 in-situ particulate composite synthesized in open hearth furnace with manually controlled stirring method.” International journal of advanced materials manufacturing & characterization, 3: 227-230, 2013.

[8] Michael Rajan H.B., S. Ramabalan., I .Dinaharan., S. J. Vijay., “Effect of TiB_2 content and temperature on sliding wear behavior of AA7075/TiB_2 in situ aluminum cast composites”, Archives of Civil and Mechanical Engineering, 4(1):72-79, 2014.

[9] Hani Henein., Hulya Kaftelen., Necip Unlu., Gultekin Goller., M. Lutfi Ovecoglu., “Comparative processing-structure-property studies of Al-Cu matrix composites reinforced with TiC particulates”, Materials and design, 812-824, 2011.

[10] H. Assadi., S.A. Alidokht., A. Abdollah-Zadeh., “Effect of applied load on the dry sliding wear behaviour and the subsurface deformation on hybrid metal matrix composite”, Materials and design, 305: 291-298, 2013.

[11] Ali Mazahary., Mohsen Ostad Shabani., “Study on microstructure and abrasive wear behaviour of sintered Al matrix composite”, Ceramics International, 38: 4263-4269, 2012.

[12] Shrinath Viswanathan., Durbadal Mandal., “Effect of re-melting on particle distribution and interface in SiC reinforced 2124Al matrix composite”, Materials and design, 86: 21-27, 2013.

[13] Aleksandar Vencl., Saioa Arostegue., Aleksandar Marinkovic., Miroslav Babic., Biljana Bobic., “Structural, mechanical and tribological properties of A356 aluminium alloy reinforced with Al_2O_3, SiC and SiC + graphite particles”, Journal of alloy and compounds, 506: 631-639, 2010.

[14] Ravindra Singh Rana., Rajesh Purohit., Anil kumar Sharma., Saraswati Rana., “Optimization of Wear Performance of Aa 5083/10 Wt. % Sicp Composites Using Taguchi Method.” 3rd International Conference on Materials Processing and Characterisation (ICMPC), Procedia Materials Science, 6: 503 -511, 2014.

[15] N. Natarajan, S. Vijayarangan, I. Rajendran, “Wear behaviour of A356/25SiCp aluminium matrix composites sliding against automobile friction material”, Wear, 261: 812-822, 2006.